

UDC 620.179.16:620.178.7:620.178.151.22

EVALUATION OF MICROSTRUCTURE AND MECHANICAL PROPERTIES OF HIGH-STRENGTH BAINITIC CAST IRON USING AN ELECTROMAGNETIC SENSOR

M. Kashefi,^{1,3} M. H. Nateq,^{1,4} and S. Kahrobaee²

Translated from *Metallovedenie i Termicheskaya Obrabotka Metallov*, No. 6, pp. 17 – 21, June, 2017.

High-strength bainitic cast iron is studied after isothermal hardening at 340°C for from 0.5 to 5 h with the use of a non-destructive eddy-current method for monitoring the microstructure and mechanical properties. Iron microstructure is studied by optical microscopy and x-ray diffraction analysis. Brinell hardness and the impact energy are determined. Correlation is established between electromagnetic sensor signal, microstructure, and mechanical properties. It is shown that induced voltage and normalized impedance may be used for non-destructive monitoring of the production process and cast iron quality.

Key words: bainitic cast iron, eddy-current test, austenite-ferrite microstructure.

INTRODUCTION

In the last twenty years there has been a rapid increase in use of bainitic cast iron in various industries: automobile and mining; railway transport; agriculture, etc. World production of bainitic cast increased by a factor of five during 1995 – 2005 [1]. Apart from such advantages as lower manufacturing cost and weight than other cast irons [2], bainitic material has strength and toughness commensurate with these indices for steel [3]. This favorable combination of mechanical properties is due to the special microstructure called ausferrite that is a mixture of austenite and ferrite stabilized by an increase of carbon within it [4]. As a result a significant effect of heat treatment regime on final cast iron properties strict control is required for isothermal hardening for ausferrite [3].

Isothermal hardening for preparing an austenite-ferrite mixture commences with austenitizing high-strength cast iron in the range 850 – 950°C with exposure for about one hour in order to prepare a uniform austenitic structure. Then the cast iron is rapidly cooled to a temperature in the range 200 – 400°C, called the austenite tempering temperature

(T_{Aus}), subjected to isothermal exposure lasting t_{Aus} , and cooled to room temperature [5]. The isothermal quenching temperature T_{Aus} is selected proceeding from the level of final properties, and therefore the time of isothermal exposure t_{Aus} is a critical parameter. The value of T_{Aus} should be in a “process window” in order to prepare the greatest amount of austenite-ferrite mixture and correspondingly the best mechanical properties [6]. The process window depends on many factors: cast iron chemical composition, alloying element segregation, austenitizing temperature and time; isothermal quenching temperature [7]. As a result of this choice of the process window is difficult and may lead to erroneous results, and use of a sampling method and errors occupy considerable time and facilities. Bainitic cast iron consists of several phases with different magnetic properties, and therefore non-destructive methods for monitoring are sensitive to its microstructure and their use makes it possible to determine a process window precisely, and also to reveal rapidly specimens with an undesirable microstructure. Non-destructive monitoring methods are convenient for evaluating the quality of all prepared objects in mass production lines.

A good correlation has been established in [8] between the signal of magnetic Barkhausen noise and bainitic cast iron heat treatment parameters. The Barkhausen noise method has been used in order to evaluate the change in mechanical properties with variation of cast iron microstructure [9].

The aim of the present work is to evaluate the possibility of using an eddy current method for determining the micro-

¹ Department of Materials Science and Metallurgical Engineering, Engineering Faculty, Ferdowsi University of Mashhad, Mashhad, Iran.

² Department of Materials Engineering, Sadjad University of Technology, Mashhad, Iran.

³ E-mail: m-kashefi@um.ac.ir.

⁴ E-mail: mh.nateq@gmail.com.

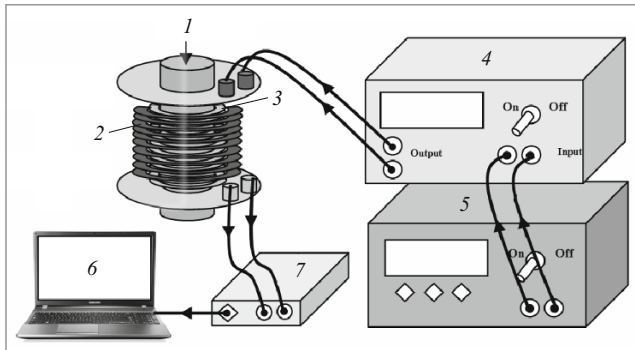


Fig. 1. Eddy current sensor layout: 1) sample; 2) excitation coil, 400 turns; 3) measuring coil, 500 turns; 4) power amplifier; 5) function generator; 6) data acquisition; 7) analog card.

structure and properties of bainitic cast iron and choice based on this of a process window for its treatment.

METHODS OF STUDY

Unalloyed high-strength cast iron of the following was studied, wt. %: 3.6 C; 2.5 Si; 0.4 Mn; 0.01 P; 0.01 S.

Eight specimens 21 mm in diameter and 120 mm long were prepared. All specimens were austenitized at 900°C for 1 h, transferred to a salt bath at 340°C where they were held for different times: $t_{\text{Aus}} = 30, 60, 90, 120, 150, 180, 240,$ and 300 min. Specimens were air cooled after exposure.

Brinell hardness and Charpy impact strength were measured for cast iron specimens according to the ASTM A327 standard. Average impact strength was determined from results of three tests.

Metallographic and X-radiographic analyses of the cast iron were conducted in order to measure the content of graphite, martensite, and austenite. The proportion of graphite was determined in polished unetched specimens. In order to evaluate martensite concentration hot etching in sodium picrate was carried out [10]. The volume fraction of austenite was calculated from the ratio of x-ray line intensity [11]. The proportion of ferrite was determined as the remaining part.

Eddy current tests were performed for all specimens at room temperature and a coil filling coefficient of 0.98. Encircling coils were used with an internal diameter of 21.2 mm and length 50 mm, the number of turns was 500 in the primary (exciting) winding and 650 in the second (recording) winding. A sinusoidal current frequency of 400 Hz was used. Recording of the induced voltage and standard impedance (electrical resistance alternating current) was recorded. The eddy current system is shown in Fig. 1.

RESULTS AND DISCUSSION

Changes in cast iron microstructure during isothermal transformation occur in two stages.

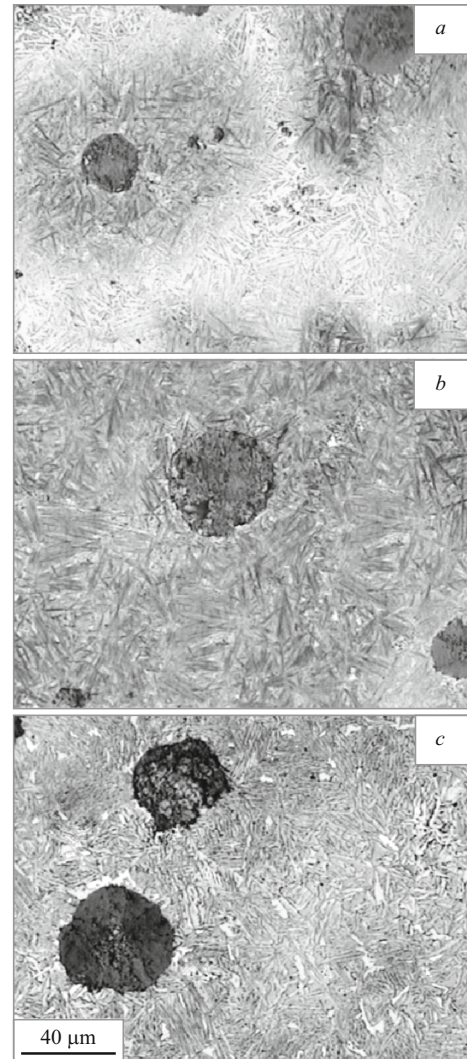


Fig. 2. High-strength bainitic cast iron microstructure after isothermal soaking at 340°C for 30 min (a), 150 min (b), and 300 min (c).

In the first stage the original metastable austenite (γ_i) formed during austenitizing starts to be converted into a mixture of ferrite and austenite (ausferrite); the two-phase microstructure formed is dispersed acicular ferrite (α_{ac}) in a matrix of high-carbon stabilized austenite (γ_{hc}). The structure obtained increases cast iron strength and impact toughness considerably [12]. During ferrite generation carbon diffuses in austenite. Austenite enriched in carbon becomes stable at room temperature. This process commences close to graphite nodules and propagates further into the matrix during the whole isothermal exposure period. Inadequate duration of isothermal exposure t_{Aus} leads to incomplete decomposition of the remaining original low-carbon austenite. This austenite, unstable at room temperature, is transformed into martensite during subsequent cast iron cooling. A cast iron microstructure is shown in Fig. 2a after isothermal exposure $t_{\text{Aus}} = 30$ min. It is seen that after austenite formation around graphite nodules in areas where previously there was

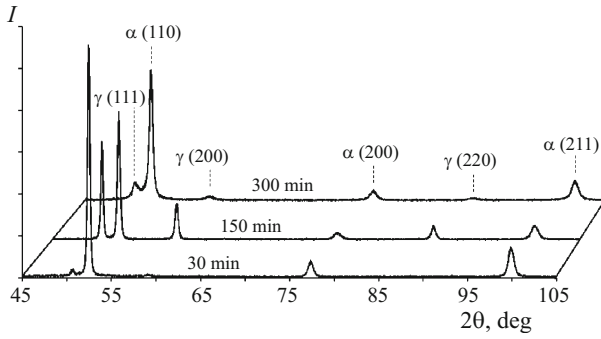


Fig. 3. High-strength cast iron diffraction pattern after isothermal soaking of specimens for 30, 150, and 300 min.

low-carbon austenite, a martensite network forms. With an increase in cast iron exposure time to 150 min complete decomposition of the original austenite proceeds with formation of solely an austenite-ferrite mixture without martensite (Fig. 2b). Therefore, with adequate isothermal exposure time it is possible to void formation of undesirable martensite.

With a further increase in exposure time a second stage of isothermal transformation commences, within which high-carbon stabilized austenite is converted into ferrite (not acicular) containing carbide precipitates [12]. A cast iron structure shown in Fig. 2c prepared with $t_{Aus} = 300$ min that is called bainitic ferrite.

Diffraction patterns of test specimens are given in Fig. 3. The lower intensity of austenite lines for specimens after exposure for 30 and 300 min points to presence within them of martensite and carbide precipitates, and both of these factors correspond to a reduction in austenite content. Martensite and carbide phase, contained even in a small amount, lead to a marked reduction in cast iron mechanical properties. In view of this the duration of isothermal exposure should be selected carefully: to provide austenite decomposition (stage 1), but not permit formation of iron carbide (stage 2).

The optimum time interval for isothermal exposure determines the “process window”. It is seen from Fig. 4a that with $t_{Aus} = 150$ min the process is still in stage 1 due to presence of martensite. In this stage the amount of high-carbon austenite and ferrite increases steadily, i.e., there is an increase in the proportion of austenite-ferrite mixture. In addition, according to Fig. 4b for these specimens impact energy increases and hardness decreases. For an exposure duration in the range $150 \leq t_{Aus} \leq 180$ min there is martensite within the structure and the amounts of austenite and ferrite are approximately constant. This range in the process window. It has been shown that in this window cast iron has the best value of impact energy (Fig. 4b). If the exposure time is more than 1280 min, the amount of ferrite starts to increase again and the austenite starts to decrease since austenite is converted into bainitic ferrite in stage 2. These processes lead to a significant reduction in impact energy.

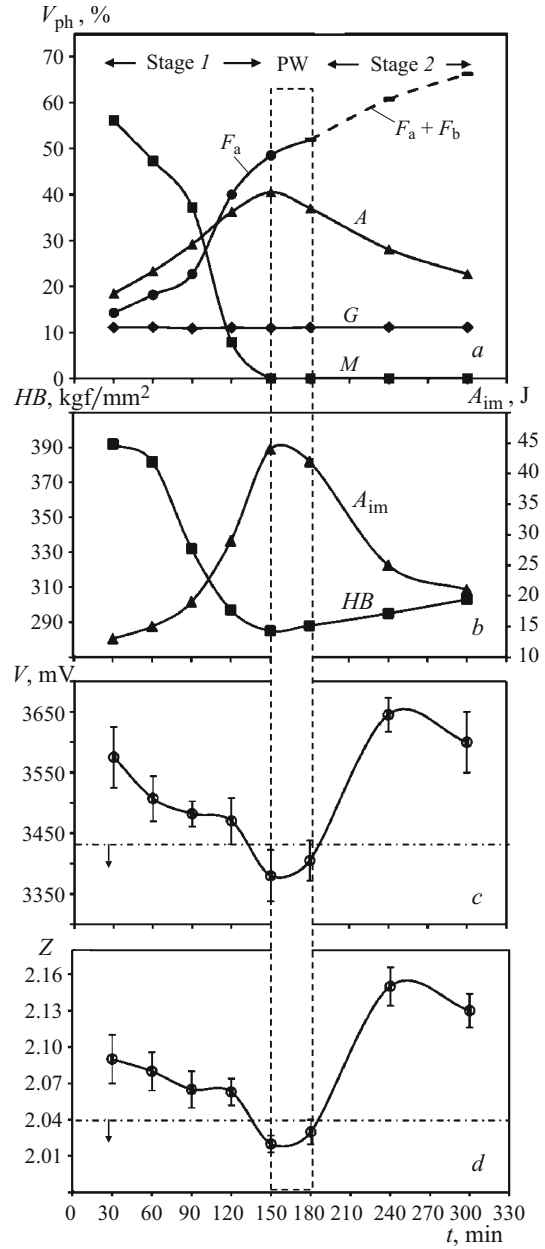


Fig. 4. Dependence of phase ratio (a), impact energy A_{im} , and hardness HB (b), induced stresses V (c), of normalized impedance Z (d) on isothermal soaking time for high-strength bainitic cast iron: PW is process window; G is graphite; A is austenite; F_a is acicular ferrite; F_b is bainitic ferrite; M is martensite.

Alternating current in a coil generates a fluctuating electromagnetic field determining coil voltage and impedance. By placing a sample in the coil an electric field is obtained within it. The eddy current itself forms a secondary electromagnetic field, opposite to the first and varying in voltage. A corresponding change in impedance and voltage in a winding is recorded by an oscillography as the output eddy signal (Fig. 1). For each specimen the output signal will be different in relation to its electromagnetic properties and winding pa-

rameters [13]. The following equations gives the ratio between electromagnetic parameters

$$Z = \sqrt{X_L^2 + R^2} = V/I; \quad (1)$$

$$X_L = 2\pi fL; \quad (2)$$

$$L = \mu N^2 A/l, \quad (3)$$

where Z is impedance (total resistance of alternating current); X_L is reactance (reactive resistance), imaginary part of total impedance signal; R is electric resistance, active part of total impedance; V is induced voltage in a coil; I is current strength; f is applied current frequency; L is coil inductance; μ is magnetic permeability; N is number of turns in a coil; A is coil cross section; l is coil length.

On condition that coil parameters are constant, at a given frequency the difference of R and μ for specimens is determined by the output signal of the eddy current sensor. For ferromagnetic materials the range of change in magnetic permeability μ is much greater than the region for the change in electrical resistance R [14, 15] and therefore the output signal of the eddy current sensor may only be interpreted on the basis of measuring its permeability. Measurement of eddy current signal at a frequency of 400 Hz for all specimens is given in Fig. 4c and d. It is seen that with a holding time of less than 150 min apart from an increase in impact energy and a reduction in hardness there is some reduction in eddy current signal. Then there is an interval of durations corresponding to the process window. Here the minimum values of eddy current signals coincide with the greatest values of impact energy and least hardness values. With durations of isothermal exposure more than 180 min the output signal shows an oscillatory tendency outside a visible connection with mechanical properties. In order to analyze results it is necessary to consider the effect of isothermal exposure duration mainly on magnetic permeability. Output signals Z and V are proportional to μ according to Eqs. (1) – (3). In stage 1 when the exposure time is less than 150 min, the increase in amount of magnetized austenite with $\mu = 1$ leads to reduction in overall specimen permeability and correspondingly a reduction in eddy current signal. In contrast, a reduction in the proportion of martensite and an increase in amount of ferrite causes an increase in magnetic permeability since that for ferrite is greater than for martensite. As a result of this the rate of reduction in eddy current signal slows down.

Similar interpretation is also applicable to the regime in the duration window. The maximum amount of austenite determines the least values of eddy current signal. A broken-dotted (horizontal) line (Fig. 4c and d) shows (in the direction of an arrow) suitable specimen treatment regimes in the duration window for obtaining favorable mechanical properties.

Conditions are different in stage 2. Ferrite is the single ferromagnetic component, its amount increases, and the

amount of non-magnetic austenite decreases. Both of these factors lead to a general increase in specimen magnetic permeability. However, carbide particles that develop act as a hindrance to domain boundary movement [16], which facilitates a reduction in overall specimen permeability. As is seen from Fig. 4c and d, the effect of carbide increases with an increase in exposure time, and therefore the change in eddy current signal becomes oscillatory.

CONCLUSIONS

An output eddy current signal (normalized impedance and induced voltage) is sensitive to phase transformation during isothermal hardening of high-strength bainitic cast iron. Signal variation with different isothermal exposure time agrees with a change in microstructure and mechanical properties (impact energy and hardness). Therefore, a non-destructive eddy current method makes it possible to reveal cast iron specimens with the best mechanical properties.

REFERENCES

1. A. Rimmer, "ADI solutions aid vehicle design," *Foundry Trade J.*, **1**, 54 – 56 (2004).
2. K. L. Hayrynen "ADI: Another Avenue for ductile iron foundries," *Modern Casting*, **85**, 35 – 38 (1995).
3. R. Ellio, M. Bahmani, and N. Varahram, "Austempered ductile iron: A competitive alternative for rapid induction hardened steel crankshaft," *Cast Metals*, **9**, 249 – 257 (1997).
4. B. V. Kovacs, "On the terminology and structure of austempered ductile iron," *AFS Trans.*, **102**, 417 – 420 (1994).
5. K. L. Hayrynen, K. R. Brandenburg, and J. R., Keuogh, "Application of austempered ductile irons," *AFS Trans.*, **110**, 1 – 10 (2002).
6. T. N. Rouns and K. B. Rundman, "Constitution of austempered ductile iron and kinetics of austempering," *AFS Trans.*, **95**, 871 – 874 (1987).
7. R. C. Voigt and C. R. Loper, "Austempered ductile iron: Process control and quality assurance," *J. Heat Treat.*, **3**, 291 – 309 (1984).
8. C. D'Amato, C. Verdu, X. Kleber, G. Regheere, and A. Vincent, "Characterization of austempered ductile iron through Barkhausen noise measurements," *J. Nondestr. Eval.*, **22**, 127 – 139 (2003).
9. C. H. Gur, M. Ozer, and M. Erdogan, "Investigation of the variations in microstructure and mechanical properties of dual matrix ductile iron by magnetic Barkhausen noise analysis," *Res. Nondestr. Eval.*, **19**, 44 – 60 (2008).
10. H. Tian and D. M. Stefanescu, "Application of a coloration etching method to the study of microstructures in primary and eutectic solidification in cast iron," *Mater. Charact.*, **3**, 329 – 333 (1992).
11. O. Eric, M. T. Jovanovic, L. Sidjanin, and D. Rajnovic, "Microstructure and mechanical properties of CuNiMo austempered ductile iron," *J. Min. Metall.*, **40**, 11 – 19 (2004).
12. M. Baydogan and H. Cimenoglu, "The effect of austempering time on mechanical properties of a ductile iron," *Scand. J. Metall.*, **30**, 391 – 395 (2001).

13. M. H. Nateq, M. Kashefi, and S. Kahrobaee, "Use of eddy-current method for determining the thickness of induction-hardened layer in cast iron," *Metall. Sci. Heat Treat.*, **55**, 370 – 374 (2013).
14. L. Kh. Kogan, "Effect of the carbon content on the magnetic and electric properties of thermally treated carbon steels and the possibilities of testing the quality of tempering of articles produced from them via the eddy-current method," *Russ. J. Nondestr. Test.*, **42**, 616 – 629 (2006).
15. M. Johnson, C. Lo, S. Hentscher, and E. Kinser, "Analysis of conductivity and permeability profiles in hardened steel," in: L. Udpa and N. Bowler (eds.), *Electromagnetic Non-Destructive Evaluation (IX)*, IOS, Amsterdam (2005).
16. M. Kashefi and S. Kahrobaee, "Determination of presence of undesirable carbides at surface of cast iron parts using differential eddy current technique," *Mater. Sci. Technol.*, **29**, 990 – 994 (2013).